Texture in Digital Breast Tomosynthesis: A Comparison between Mammographic and Tomographic Characterization of Parenchymal Properties

Despina Kontos, Predrag R. Bakic and Andrew D.A. Maidment
University of Pennsylvania, Department of Radiology, 3400 Spruce St., Philadelphia PA 19104
{Despina.Kontos | Predrag.Bakic| Andrew.Maidment} @uphs.upenn.edu

ABSTRACT

Studies have demonstrated a relationship between mammographic texture and breast cancer risk. To date, texture analysis has been limited by tissue superimposition in mammography. Digital Breast Tomosynthesis (DBT) is a novel x-ray imaging modality in which 3D images of the breast are reconstructed from a limited number of source projections. Tomosynthesis alleviates the effect of tissue superimposition and offers the ability to perform tomographic texture analysis; having the potential to ultimately yield more accurate measures of risk. In this study, we analyzed texture in DBT and digital mammography (DM). Our goal was to compare tomographic versus mammographic texture characterization and evaluate the robustness of texture descriptors in reflecting characteristic parenchymal properties. We analyzed DBT and DM images from 40 women with recently detected abnormalities and/or previously diagnosed breast cancer. Texture features, previously shown to correlate with risk, were computed from the retroareolar region. We computed the texture correlation between (i) the DBT and DM, and (ii) between contralateral and ipsilateral breasts. The effect of the gray-level quantization on the observed correlations was investigated. Low correlation was detected between DBT and DM features. The correlation between contralateral and ipsilateral breasts was significant for both modalities, and overall stronger for DBT. We observed that the selection of the gray-level quantization algorithm affects the detected correlations. The strong correlation between contralateral and ipsilateral breasts supports the hypothesis that parenchymal properties appear to be inherent in an individual woman; the texture of the unaffected breast could potentially be used as a marker of risk.

Keywords: Feature extraction, Quantitative image analysis; Mammography, Digital breast tomosynthesis; Risk assessment.

1. INTRODUCTION

Parenchymal patterns are the mammographic visual effect of breast density; parenchymal patterns in x-ray breast images are formed by the distribution of fatty, glandular, and stromal breast tissues [1, 2]. While the relationship between mammographic breast density and breast cancer risk has been clearly demonstrated [3], studies have also shown that a potential relationship exists between mammographic parenchymal texture and the risk of developing breast cancer [4-6]. Texture features extracted particularly from the retroareolar breast region appear to have the best performance in distinguishing between women at different breast cancer risk levels [7, 8]. These studies suggest that computer-extracted texture features, could provide fully-automated, objective, and reproducible methods to identify parenchymal patterns that are associated with increased levels of risk.

Mammograms, however, are 2D images that visualize a compressed projection of the 3D breast volume (Fig. 1.a). Therefore, texture features computed from mammograms reflect the properties of superimposed breast tissues, including the skin and the surrounding subcutaneous fat layers. Knowing that the risk for developing breast cancer is mainly associated with properties of the fibroglandular tissue (*i.e.* breast density), layers such as the skin or subcutaneous fat could be considered as anatomical noise in terms of image-based risk characterization. Considering these limitations of mammography, tomographic breast imaging could provide better means to perform parenchymal texture analysis, and ultimately yield more accurate measures for breast cancer risk estimation.

Medical Imaging 2008: Computer-Aided Diagnosis, edited by Maryellen L. Giger, Nico Karssemeijer
Proc. of SPIE Vol. 6915, 69150A, (2008) · 1605-7422/08/$18 · doi: 10.1117/12.773144

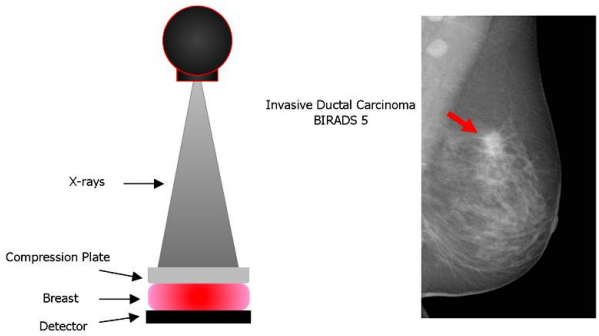

(a) Digital Mammography

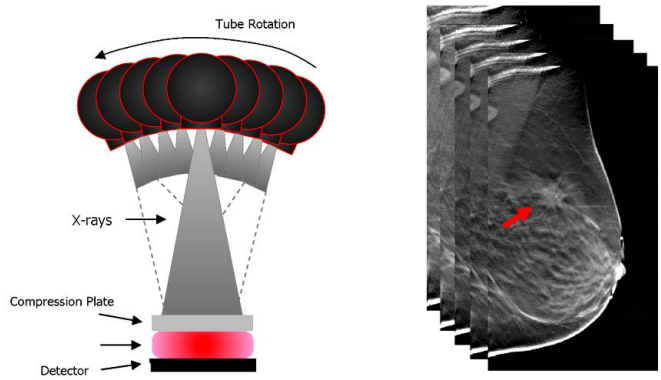

(b) Digital Breast Tomosynthesis

Fig. 1 Imaging geometry and lesion conspicuity with (a) DM and (b) DBT

Digital breast tomosynthesis (DBT) is a novel 3D x-ray imaging modality in which tomographic images of the breast are reconstructed from multiple low-dose x-ray source projection images acquired at different angles of the x-ray tube [9] (Fig. 1.b). By combining information from different projections, tomosynthesis filters out non-adjacent anatomical breast structures, alleviating the effect of tissue superimposition. Clinical trials have shown that tomosynthesis provides superior tissue visualization and improved lesion conspicuity in comparison to projection mammography, resulting in higher sensitivity and specificity [10, 11]. Having the advantage of tomographic imaging, DBT offers the potential to alleviate the effect of tissue superimposition in parenchymal analysis, which could result in more accurate texture measures for breast cancer risk estimation.

In this study, we analyzed texture in DBT and digital mammography (DM); we computed texture features that have been shown in previous studies with mammograms to correlate with breast cancer risk [4-8]. Our goal was to compare tomographic versus mammographic texture characterization and evaluate the robustness of the texture descriptors in reflecting characteristic parenchymal properties. This study extends our previous report on texture analysis in tomosynthesis source projection images [12]. Parenchymal analysis was performed in the retroareolar breast region using computer-extracted texture features. We computed the correlation between mammographic and tomographic texture features. The degree of this correlation indicates the extent in which tissue superimposition introduces differences in image texture between the two modalities. We also computed the correlation of the texture features between the contralateral and ipsilateral breast of each woman. The degree of similarity in parenchymal texture between the affected and unaffected breasts reflects the degree to which characteristic parenchymal properties are inherent in an individual woman. This is an essential assumption in order to consider parenchymal texture as a marker of risk: The underlying hypothesis is that inherent biological factors associated with the risk of developing breast cancer are expressed in a woman's parenchymal tissue and subsequently manifested in her mammographic texture [13].

Our long-term hypothesis is that DBT parenchymal analysis could provide more accurate texture measures for image-based breast cancer risk estimation; our goal is to develop DBT texture biomarkers that can be used to provide Computer-Assisted Risk Estimation (CARe) of breast cancer in clinical practice.

2. METHODS

2.1. Dataset

The images included in our analysis have been retrospectively collected from a clinical multimodality breast imaging study that has been completed in our department (NIH R01 CA85484-01A2). We analyzed bilateral DBT and DM images from 40 women with recently detected abnormalities and/or previously diagnosed breast cancer (mean age 51.4 years, average Gail risk 11%). DBT and DM acquisition was performed on the same day with a GE Senographe 2000D FFDM (General Electric Medical Systems, Milwaukee, WI) system, modified to allow positioning of the x-ray tube at 9 locations by varying the angle from -25° to +25° with increments of 6.25°. The breast was compressed in an MLO position and the source images were acquired with spatial resolution of 100 μm/pixel. Filtered-backprojection was used to reconstruct DBT tomographic planes in 1mm increments with 0.22mm in-plane resolution. Retroareolar $(2.5\ \text{cm})^3$ ROIs were manually segmented from the DBT reconstructed images; corresponding $(2.5\ \text{cm})^2$ ROIs were segmented from the *Premium View*™ DM images. Three ROIs with technical image artifacts were excluded from the analysis; one segmented from a breast contralateral to cancer and two segmented from breasts ipsilateral to cancer.

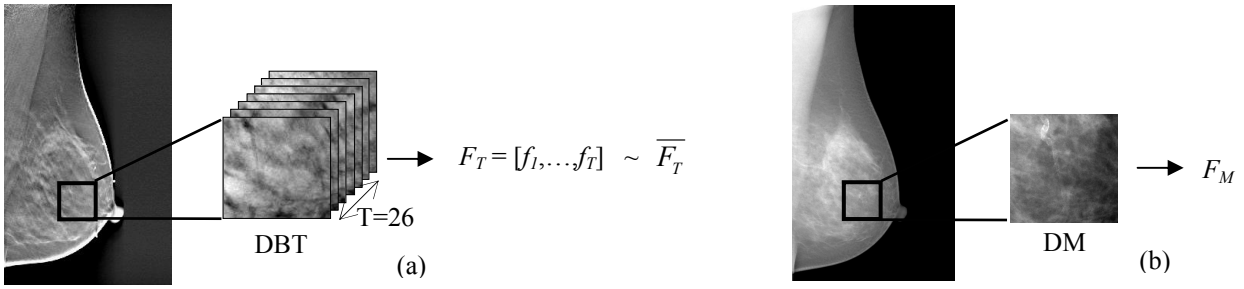

Fig. 2 An example of (a) DBT ROI and the average DBT texture feature $\overline{F_T}$ and (b) the corresponding DM ROI with the single-valued DM texture feature F_M.

2.2. Texture feature extraction

Texture features of skewness, coarseness, contrast, and energy were estimated. These features have been shown in previous studies with mammograms to correlate with the risk of developing breast cancer [4-6, 8]. For each texture descriptor, we computed a feature f_i, i=1,…,T from each tomographic plane (T=26 slices in each ROI, 1mm/slice), resulting to a feature vector $F_T = [f_1,\ldots,f_T]$ for each DBT ROI (Fig. 2.a). The mean of the feature vector, $\overline{F_T}$ was used as the representative feature for the ROI. Single-valued texture features F_M were computed from the corresponding 2D DM ROI (Fig. 2.b).

Skewness reflects the properties of the gray-level histogram and has been used to assess parenchymal density [5, 6]. When the image texture is predominantly composed of fat (*i.e.* the grey-level histogram is skewed to higher values) the skewness tends to be positive, whereas when the texture is primarily formed by dense tissue (*i.e.* the gray-level histogram is skewed to lower values) the skewness values tend to be negative. Skewness is the third statistical moment, computed as:

$$skewness = \frac{w_3}{w_2^{3/2}} \quad , \quad \text{where} \quad w_k = \sum_{i=0}^{g_{\max}} n_i (i-\bar{i})^k / N \quad , \quad N = \sum_{i=0}^{g_{\max}} n_i \quad , \quad \bar{i} = \sum_{i=0}^{g_{\max}} (i n_i / N) \quad ,$$

and n_i represents the number of times that gray level value i takes place in the image region, g_{max} is the maximum gray-level value and N is the total number of image pixels.

Coarseness is a texture feature that reflects the local variation in image intensity; small coarseness value for an ROI indicates fine texture, where the gray levels of neighboring pixels are different; high coarseness value indicates coarse texture, where neighboring pixels have similar gray level values. Coarseness computation is based on the Neighborhood Gray Tone Difference Matrix (NGTDM) [5, 14] of the gray-level values within the image region.

$$coarseness = \left(\sum_{i=0}^{g_{\max}} p_i v(i) \right)^{-1}, \quad \text{where} \quad v(i) = \begin{cases} \sum | i - \bar{L}_i | \; for \; i \in \{n_i\} \; if \; n_i \neq 0 \\ 0 \quad otherwise \end{cases} \text{ is the NGTDM}$$

In the above formulas, g_{max} is the maximum gray-level value, p_i is the probability that gray level i occurs, $\{n_i\}$ is the set of pixels having gray level value equal to i, and $\overline{L_i}$ is given by

$$\bar{L}_i = \frac{1}{S-1} \sum_{k=-t}^{t} \sum_{l=-t}^{t} j(x+k, y+l),$$

where $j(x,y)$ is the pixel located at (x,y) with gray level value i, $(k,l) \neq (0,0)$ and $S=(2d+1)^2$ with d specifying the neighborhood size around the pixel located at (x,y).

Contrast and Energy, as proposed originally by Haralick [15], require the computation of a gray-level co-occurrence matrix, which is based on the frequency of the spatial co-occurrence of gray-level intensities in the image. Contrast quantifies overall variation in image intensity, while energy is a measure of image homogeneity.

$$contrast = \sum_{i}^{g} \sum_{j}^{g} |i - j|^2 C(i,j), \quad \text{and} \quad energy = \sum_{i}^{g} \sum_{j}^{g} C(i,j),$$

where g is the total number of different gray levels and C is the normalized co-occurrence matrix [15].

2.3. Gray-level quantization

In our dataset, the DBT gray-level values ranged on average between N_{min}=1388 and N_{max}=9033 for each ROI; the corresponding DM gray-level values ranged between N_{min}=2074 and N_{max}=2679. Due to the large range of gray-level values in DBT, gray-level quantization becomes essential for calculating contrast and energy. The large range of gray-level values results in large sparse co-occurrence matrices and un-reliable co-occurrence texture statistics [15, 16]. In addition, the computational cost for calculating the co-occurrence matrix for contrast and energy becomes prohibitive [15, 16].

Two quantization algorithms were implemented, denoted by Q_C and Q_R. In both algorithms, the range of the original gray-level values N_g in each ROI was linearly scaled down to a smaller range of N_G gray-level values (*i.e.* $N_G < N_g$). The way that N_G was defined for each ROI was different in each of the two quantization algorithms:

(i) In Q_C all the ROIs where quantized to the <u>*same number*</u> of gray-levels. A range of different values for N_G was tested during the experiments, and was equal to:

$N_G^{DBT} = \{16, 32, 64, 128, 256, 512, 1024, 2048\}$ for DBT and, $N_G^{DM} = \{16, 32, 64, 128\}$ for DM.

(ii) In Q_R all ROIs were quantized to the <u>*same degree*</u>; each ROI was quantized relative to its original range of gray-level values N_g. A range of different values for N_G was tested during the experiments, and was equal to:

$N_G^{DBT} = \{ N_g/4, N_g/8, N_g/16, N_g/32, N_g/64, N_g/128\}$, and $N_G^{DM} = \{ N_g, N_g/2, N_g/4, N_g/8, N_g/16, N_g/32, N_g/64, N_g/128\}$.

2.4. Data analysis

The goal of our analysis was to compare tomographic and mammographic texture characterization and to evaluate the robustness of the different texture descriptors in reflecting characteristic parenchymal properties. To evaluate the extent in which tissue superimposition introduces differences in image texture between DBT and DM, we computed the correlation between $\overline{F_T}$ and F_M texture features. To evaluate the degree in which parenchymal texture is inherent in an individual woman, texture correlation was also computed between the features of the contralateral and ipsilateral breast of each woman. The Pearson correlation coefficient (r) was used, where f_1, f_2 represent the features for which a correlation is tested.

$$r = \frac{\sum \left(f_1 - \overline{f_1}\right) \cdot \left(f_2 - \overline{f_2}\right)}{\sqrt{\sum \left(f_1 - \overline{f_1}\right)^2 \cdot \sum \left(f_2 - \overline{f_2}\right)^2}}$$

Appropriate p-values were estimated to reflect the probability of having a correlation as large as the observed value by random chance, when the true correlation is zero. The p-value was computed by transforming the r correlation coefficient into a t-statistic having n-2 degrees of freedom, where n was the number of features in each of the two groups under comparison. The confidence bounds of the p-value were approximated using an asymptotic normal distribution of $0.5\times\log((1+r)/(1-r))$, with an approximate variance equal to $1/(n-3)$. These bounds are accurate by approximation when the sample has a multivariate normal distribution. Statistical significance was set to α=0.05.

3. RESULTS

3.1. Texture correlation between DBT and DM

Overall, low correlation was observed between DBT and DM texture features. Table 1 shows the Pearson correlation coefficients between the texture features computed from each imaging modality. For contrast and energy, the average correlation is reported over the correlations detected when varying the number of quantization gray-levels N_G; the corresponding standard deviation is shown in the parenthesis. The observed low standard deviations indicate that, for each quantization algorithm (*i.e.* Q_C and Q_R), the detected correlations for contrast and energy were robust when varying the number of gray levels N_G. However, as Table 1 shows, the strength of the contrast correlation between DBT and DM was affected by the selection of the quantization algorithm; the Q_R algorithm appeared to yield stronger contrast correlation between DBT and DM. Figure 3 shows the scatter-plots of the DBT versus the DM texture features with fitted linear regression lines. For contrast and energy, representative results are shown for selected values of N_G in order to illustrate the effect of the quantization algorithm on the detected texture correlation between the two modalities.

Table 1. Pearson correlation coefficient (r) between DBT and DM texture features ('*' for p-value ≤ 0.05)

	Correlation (r)
Skewness	-0.22 *
Coarseness	0.28 *
Contrast (Q_C: N_G = {16,…,128})	0.10 (std=0.003)
Contrast (Q_R: N_G = { N_g/4,…, N_g/128})	0.41 (std=0.06) *
Energy (Q_C: N_G = {16,…,128})	0.22 (std=0.02) *
Energy (Q_R: N_G = { N_g/4,…, N_g/128})	0.22 (std=0.06) *

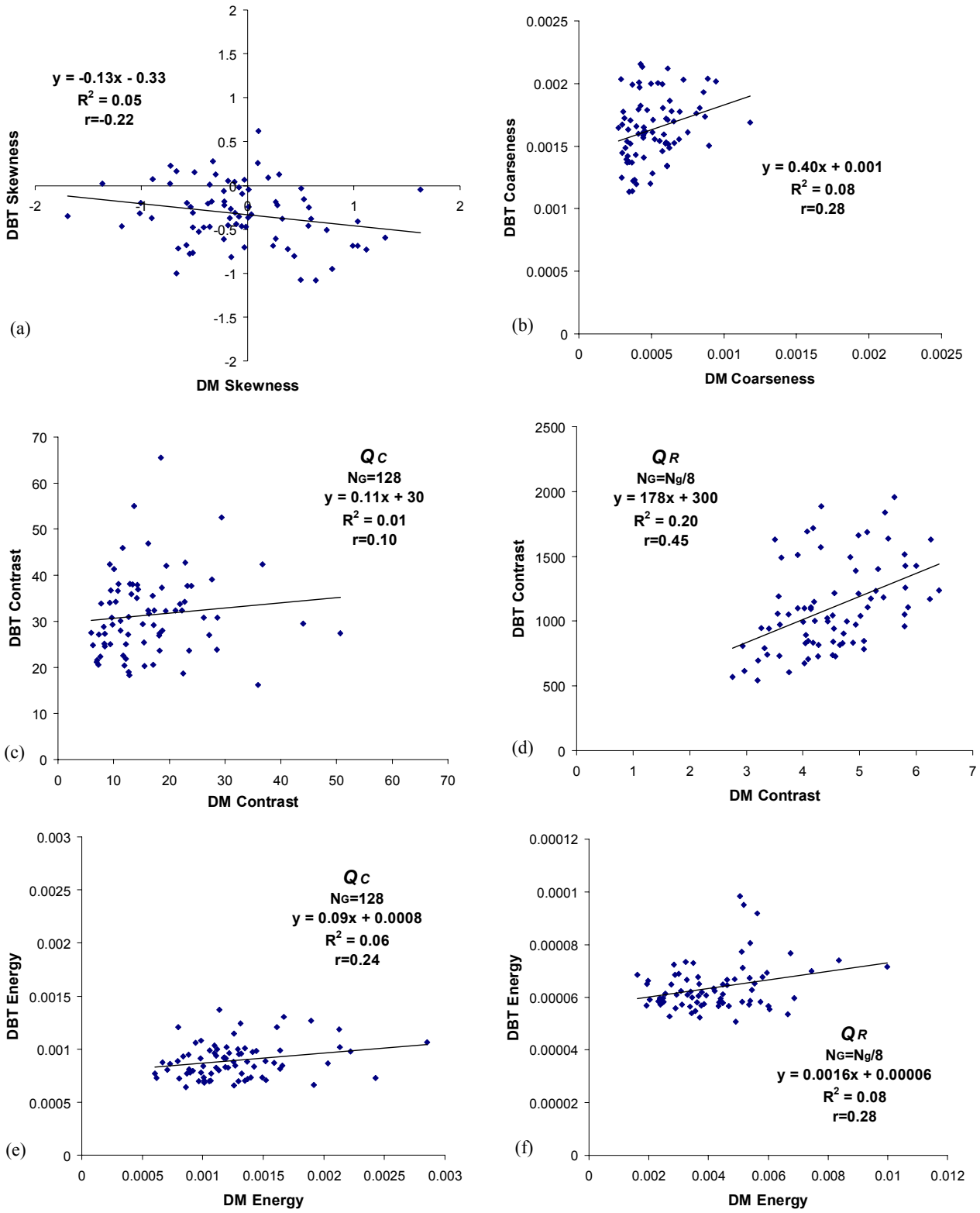

Fig. 3 Scatter-plots and fitted linear regression lines for texture features computed from DBT and DM: (a) skewness, (b) coarseness, (c) contrast for Q_C and N_G=128, (d) contrast for Q_R and N_G=N_g/8, (e) energy for Q_C and N_G=128, (f) energy for Q_R and N_G=N_g/8.

3.2. Texture correlation between contralateral and ipsilateral breasts

Strong texture correlation was detected between the contralateral and ipsilateral breast of each woman in both imaging modalities. Overall, the DBT demonstrated stronger texture between-breast correlation. Table 2 shows the Pearson correlation coefficients between the texture features computed from contralateral and ipsilateral breasts, for DBT and DM. For contrast and energy, the average correlation is reported over the correlations detected when varying the number of quantization gray-levels N_G; the standard deviation in the parenthesis indicates the variation of the correlation coefficient over the different values of N_G. Again, the observed low standard deviations indicate that the detected correlations for contrast and energy were robust, for the same quantization algorithm, when varying the number of gray levels N_G. However, as Table 2 shows, the strength of the detected correlations was affected by the selection of the quantization algorithm. The Q_R quantization algorithm appeared to yield stronger correlations than Q_C for both contrast and energy. Figure 4 shows the scatter-plots with fitted regression lines for the skewness and coarseness texture features computed from contralateral versus ipsilateral breasts, for DBT and DM. Figures 5 and 6 show representative scatter plots for contrast and energy, for selected values of N_G; illustrating the effect of the quantization algorithm on the between-breast texture correlation. As shown in Figures 4-6, for almost all texture descriptors, DBT analysis revealed stronger parenchymal texture correlation, in comparison to DM, between contralateral and ipsilateral breast.

Table 2. Pearson correlation coefficient (r) between texture features from contralateral and ipsilateral breasts ('*' for p-value ≤ 0.05)

	Correlation (r)	
	DBT	**DM**
Skewness	0.62 *	0.56 *
Coarseness	0.44 *	0.59 *
Contrast (Q_C: N_G = {16,…,128})	0.63 (std=0.00) *	0.56 (std=0.00) *
Contrast (Q_R: N_G = { N_g/4,…, N_g/128})	0.80 (std=0.00) *	0.70 (std=0.15) *
Energy (Q_C: N_G = {16,…,128})	0.29 (std=0.03)	0.29 (std=0.02)
Energy (Q_R: N_G = { N_g/4,…, N_g/128})	0.83 (std=0.13) *	0.60 (std=0.06) *

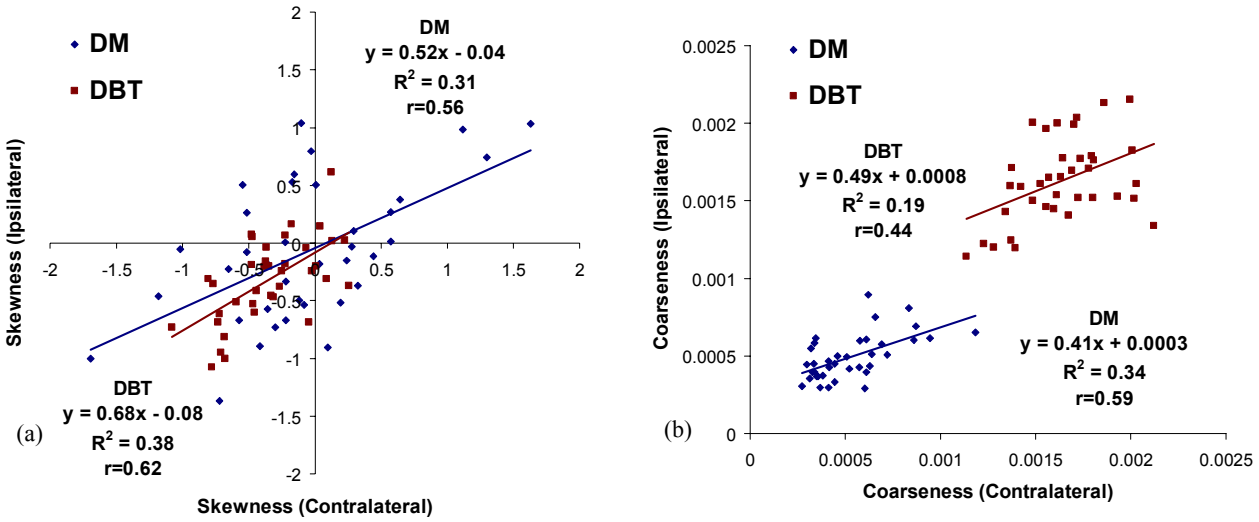

Fig. 4 Scatter-plots and fitted linear regression lines for (a) skewness and (b) coarseness computed from contralateral and ipsilateral breasts, in DBT and DM.

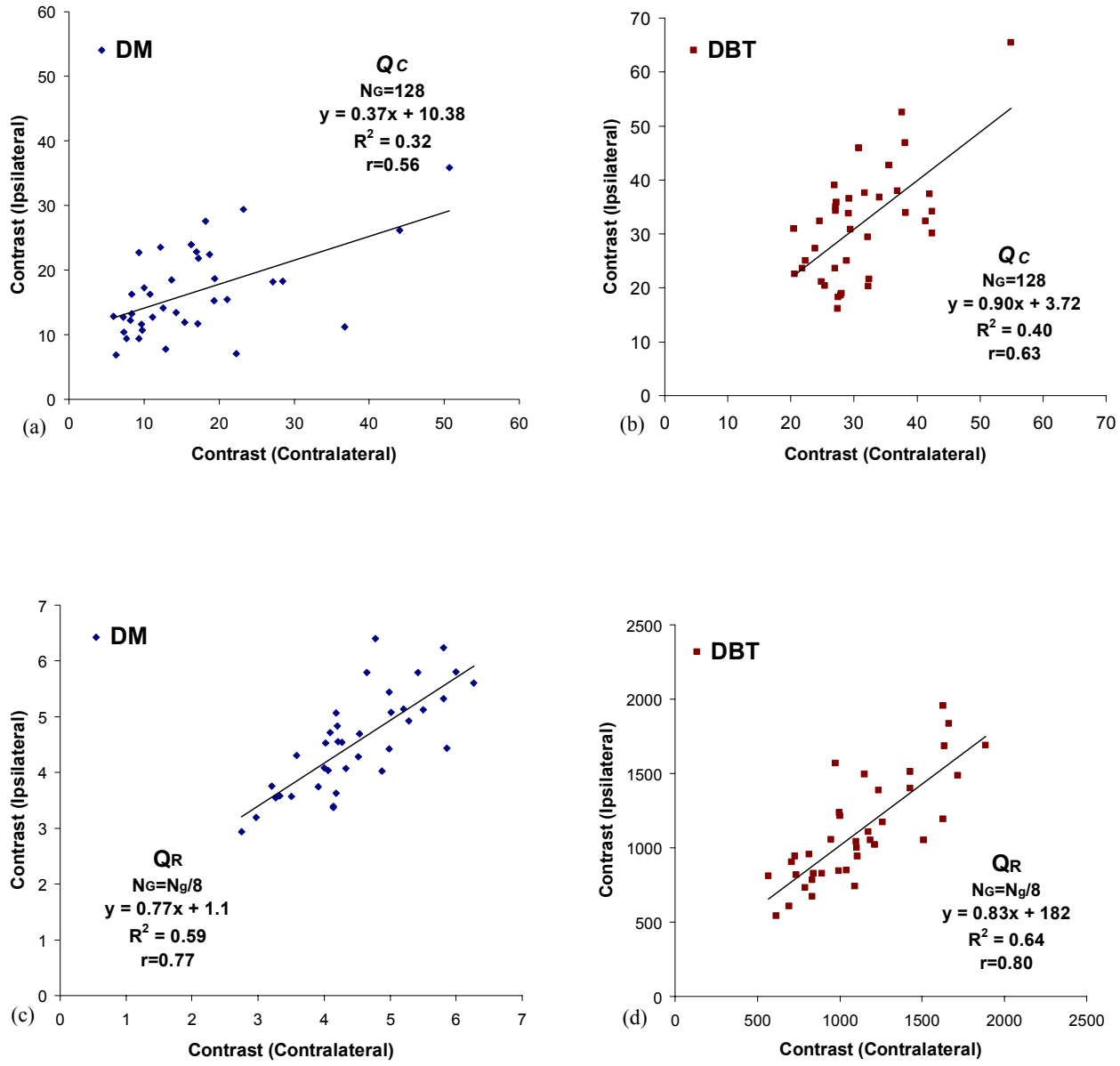

Fig. 5 Scatter-plots and fitted linear regression lines for contrast texture features computed from contralateral and ipsilateral breasts for (a) DM with Q_C and N_G=128, (b) DBT with Q_C and N_G=128, (c) DM with Q_R and N_G=N_g/8, (d) DBT with Q_R and N_G=N_g/8.

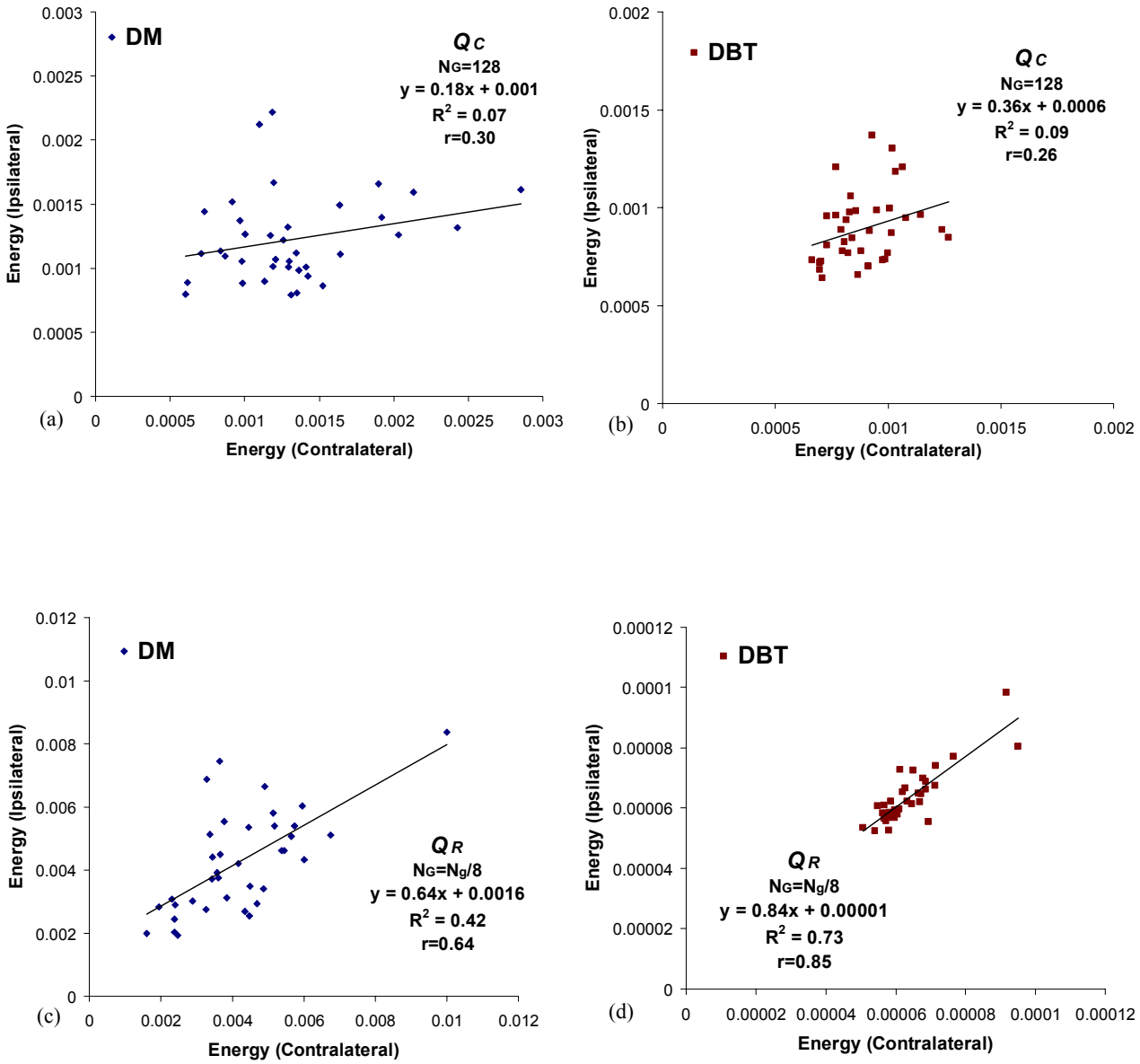

Fig. 6 Scatter-plots and fitted linear regression lines for energy texture features computed from contralateral and ipsilateral breasts for (a) DM with Q_C and N_G=128, (b) DBT with Q_C and N_G=128, (c) DM with Q_R and N_G=N_g/8, (d) DBT with Q_R and N_G=N_g/8.

4. DISCUSSION

To date, parenchymal texture has been analyzed from conventional film mammograms digitized for performing computerized analysis [4-8]; making it difficult to assess both the effect of tissue superimposition and the effect of the digitization process on the computed texture features. Here, we performed parenchymal texture analysis in DBT and DM. We computed texture features that have been shown, in previous studies with mammograms, to correlate with breast cancer risk [4-8]. Our goal was to compare tomographic versus mammographic texture characterization and evaluate the robustness of the texture descriptors in reflecting characteristic parenchymal properties.

Low correlation was observed between DBT and DM texture features, indicating that parenchymal texture differs between the two modalities. This low correlation could potentially be attributed to the effect of tissue superimposition in DM and the reconstruction algorithm in DBT; parenchymal texture is affected by both of these factors. We are particularly interested in assessing the effect of tissue superimposition. By filtering out the adjacent anatomical structures within the breast volume, DBT alleviates the effect of tissue superimposition, offering the advantage to perform tomographic texture analysis. Therefore, texture features in DBT do not reflect the properties of superimposed tissues as in DM; they reflect properties of selected spatially localized regions within the breast volume. The detected low correlation between DBT and DM shows that tomographic texture analysis in DBT provides different features, and therefore different information, compared to features extracted from projection mammography.

The correlation between contralateral and ipsilateral breasts was significant for both modalities; indicating that characteristic parenchymal properties are inherent in an individual woman. This is an essential assumption for performing image-based cancer risk estimation: the increasingly supported hypothesis is that inherent biological factors associated with the risk of developing breast cancer are expressed in a woman's parenchymal tissue and subsequently manifested in her mammographic parenchymal patterns [13, 17]. In addition, the strong between-breast correlation indicates that parenchymal texture of the unaffected breast could be used as a surrogate of risk.

Overall, the texture correlation between contralateral and ipsilateral breasts was stronger for DBT. The detected stronger between-breast correlation in DBT could be attributed to the ability to perform spatially localized texture analysis within the breast volume; while excluding tissue layers such as the skin and the surrounding subcutaneous fatty layers that introduce anatomical noise in texture characterization. If certain regions within the breast, such as the retroareolar breast region, are indeed inherent in individual women, and appear to be indicative the risk to develop breast cancer [4-8], then the ability to selectively characterize their particular texture by excluding irrelevant layers of tissue, could result in obtaining more discriminative texture features. The observed stronger between-breast texture correlation in DBT could potentially indicate this effect. Our hypothesis is that, due to the technical improvements introduced by DBT, there is a potential to capture more accurately the texture properties of characteristic breast regions, and ultimately derive more accurate measures of risk.

As part of our analyses, we also investigated the effect of gray-level quantization on co-occurrence texture features. While previous studies have used co-occurrence texture features for breast cancer risk estimation [4-8], the effect of gray-level quantization, required to compute co-occurrence statistics, has not been adequately clarified. Other studies have shown that the performance of image classification can be affected by the degree of gray-level quantization [16, 18]. In our analyses, the observed correlations for co-occurrence texture descriptors were robust when varying the number of gray-levels for image quantization; however the strength of the correlations was affected by the selection of the particular quantization algorithm. Further analysis is underway to identify the optimal gray-level quantization approach in association with the performance of the texture features in breast cancer risk estimation. Our ultimate goal is to determine the optimal texture feature extraction methodology to yield the most accurate texture measures for breast cancer risk estimation.

5. CONCLUSION

To the best of our knowledge, this is the first study to compare tomographic texture in DBT versus projection texture in DM. Texture features, previously shown to associate with risk, were computed from the retroareolar breast region. We computed the correlation between (i) the DBT and DM texture features, and (ii) between the contralateral and ipsilateral breast of each woman in both imaging modalities. The effect of the gray-level quantization on the observed correlations was also investigated. Our analysis showed low correlation between DBT and DM features. The correlation between contralateral and ipsilateral breasts was significant for both modalities; it was overall stronger for DBT. We observed

that the selection of the gray-level quantization algorithm affects the detected correlations. The ability to perform 3D texture analysis in DBT provides the basis for developing improved breast cancer risk assessment methods using 3D parenchymal analysis. Further analysis is underway for investigating the correlation between DBT features and breast cancer risk. Our long-term goal is to develop DBT biomarkers for providing Computer-Assisted Risk Estimation (CARe) of breast cancer in clinical practice.

ACKNOWLEDGEMENT

This work was funded by the Agfa/Radiological Society of North America (RSNA) Research Fellowship in Basic Radiologic Sciences (FBRS0601), by the Siemens/ Radiological Society of North America (RSNA) Research Fellow Grant (RF0707), by the Susan G. Komen Breast Cancer Foundation Research Grant (BCRT133506), and by the National Institutes of Health/National Cancer Institute Program Project Grant P01-CA85484. We would also like to thank Dr. Ann-Katherine Carton for facilitating image acquisition and Dr. Johnny Kuo for maintaining the RSNA Medical Imaging Resource Center (MIRC) image archive.

REFERENCES

[1] Kaufhold, J., Thomas, J.A., Eberhard, J.W., Galbo, C.E., Trotter, D.E., "A calibration approach to glandular tissue composition estimation in digital mammography," Medical Physics 28(8), 1867-1880 (2002).

[2] Kopans, D., [Breast Imaging], Lippincott Williams and Wilkins, Philadelphia, (2007).

[3] Boyd, N.F., Guo, H., Martin, L.J., et al., "Mammographic density and the risk and detection of breast cancer," New England Journal of Medicine 356(3), 227-236 (2007).

[4] Li, H., Giger, M.L., Olopade, O.I., Lan, L., "Fractal analysis of mammographic parenchymal patterns in breast cancer risk assessment," Academic Radiology 14(5), 513-521 (2007).

[5] Li, H., Giger, M.L., Olopade, O.I., Margolis, A., Lan, L., Chinander, M.R., "Computerized Texture Analysis of Mammographic Parenchymal Patterns of Digitized Mammograms," Academic Radiology 12, 863-873 (2005).

[6] Huo, Z., Giger, M.L., Olopade, O.I., et al., "Computerized analysis of digitized mammograms of BRCA1 and BRCA2 gene mutation carriers," Radiology 225(2), 519-526 (2002).

[7] Huo Z., Giger M.L., W.D.E., Zhong W., Cumming S., Olopade O.I., "Computerized analysis of mammographic parenchymal patterns for breast cancer risk assessment: feature selection," Medical Physics 27(1), 4-12 (2000).

[8] Li, H., Giger, M.L., Huo, Z., et al., "Computerized analysis of mammographic parenchymal patterns for assessing breast cancer risk: effect of ROI size and location," Medical Physics 31(3), 549-555 (2004).

[9] Niklason, L.T., Christian, B.T., Niklason, L.E., et al., "Digital tomosynthesis in breast imaging," Radiology 205(2), 399-406 (1997).

[10] Rafferty, E.A., "Digital mammography: novel applications," Radiologic Clinics of North America 45(5), 831-843 (2007).

[11] Poplack, S.P., Tosteson, T.D., Kogel, C.A., Nagy, H.M., "Digital breast tomosynthesis: initial experience in 98 women with abnormal digital screening mammography," American Journal of Roentgenology 189(3), 616-623 (2007).

[12] Kontos, D., Bakic, P.R., Maidment, A.D.A., "Analysis of Parenchymal Texture Properties in Breast Tomosynthesis Images," Proc SPIE Medical Imaging: Computer Aided Diagnosis 6514, (2007).

[13] Heine, J.J., Malhotra, P., "Mammographic tissue, breast cancer risk, serial image analysis, and digital mammography. Part 1. Tissue and related risk factors," Academic Radiology 9(3), 298-316 (2002).

[14] Amadasum, M., King, R., "Textural features corresponding to textural properties," IEEE Transactions on Systems Man and Cybernetics 19, 1264–1274 (1989).

[15] Haralick, R.M., Shanmugam, K., Dinstein, I., "Textural features for image classification," IEEE Transactions on Systems, Man and Cybernetics 3, 610–621 (1973).

[16] Clausi, D.A., "An Analysis of co-occurrence texture statistics as a function of grey level quantization," Canadian Journal of Remote Sensing 28(1), 1-18 (2002).

[17] Heine, J.J., Malhotra, P., "Mammographic tissue, breast cancer risk, serial image analysis, and digital mammography. Part 2. Serial breast tissue change and related temporal influences.," Academic Radiology 9(3), 317-335 (2002).

[18] Chen, W., Giger, M.L., Li, H., Bick, U., Newstead, G.M., "Volumetric texture analysis of breast lesions on contrast-enhanced magnetic resonance images," Magnetic Resonance in Medicine 58(3), 562-571 (2007).